J. Appl. Comput. Mech., 11(4) (2025) 1075-1086
DOI: 10.22055/jacm.2025.47683.4763

ISSN: 2383-4536
jacm.scu.ac.ir

Shahid Chamran University of Ahvaz

Journal of Applied and Computational Mechanics

Research Paper

RANS Study on the Impact of Equivalence Ratio on Natural Gas/Diesel-Fueled Combustion in RCCI Engine

Fathi Hamdi, Wassim Harizi, Mouldi Chrigui

University of Gabes, Laboratory of Mechanical Modeling, Energy and Materials (M2EM), National school of engineers of gabes (ENIG), Address, Gabes, 6029, Tunisia,
Email: fathi.hamdi@enig.u-gabes.tn (F.H.); wassim.harizi@enig.rnu.tn (W.H.); mouldi.chrigui@enig.rnu.tn (M.C.)

Received August 07 2024; Revised January 02 2025; Accepted for publication January 03 2025.
Corresponding author: F. Hamdi (fathi.hamdi@enig.u-gabes.tn)

Abstract. The primary reason in favor of Reactivity Controlled Compression Ignition (RCCI) is that combustion occurs at low temperature, leading to low thermal NO_x. Using the RCCI approach is highly demanded due to stringent emission laws. The main objective of this paper is to improve engine efficiency and mitigating output pollutants. This paper investigates the impact of equivalence ratio on combustion, pollutants and performances of Natural Gas/Heptane fueled combustion. A numerical model is validated by comparing the experimental results with the numerical data. The adopted equivalence ratios are ϕ = 0.3, 0.4, 0.5, 0.6, 0.7. For each case, the amount of natural gas is increased while heptane spray remains unchanged. Ansys-forte performs the simulations using RANS framework. The hybrid model Kelvin Helmholtz Rayleigh Taylor governs the spray atomization, though turbulence is pursued using the RNG K-ε model. Under an engine regime of 910 rpm, the lowest indicated specific fuel consumption is found at ϕ = 0.6. It is reduced by around 8% compared to the experiment. Keeping with ϕ = 0.6, an increase of 15% in temperature compared to experimental work (ϕ = 0.4). This change in temperature leads to a 6% reduction in CO. The combination of NG/heptane shows a large reactivity gradient. This reactivity explicitly impacts combustion duration and phasing.

Keywords: CFD, Natural gas/ heptane, RANS, KH/RT, Equivalence ratio.

1. Introduction

Internal Combustion (IC) engines are widely used for on-road and power-generation sectors. This is primarily because fossil fuels provide high energy density. Despite significant advancements in clean combustion, the consequent emissions still require thorough investigation to comply with stringent emission regulations. Reducing pollutants follows, particularly, two-way i.e. exhaust systems and combustion chamber. First, employing aftertreatment system including Lean NOx Trap (LNT), Diesel Particulate Filters (DPF), and Selective Catalytic Reduction (SCR) are of importance to reduce up to 90% of produced gases [1]. The second intervention comes through in-cylinder chamber. It has been the subject of significant state-of-the-art studies. Low Temperature Combustion (LTC) strategy is the widely adopted [2]. Combustion in LTC engines, is premixed, in some cases partially premixed, and occurs under lean condition ($\phi << 1$). LTC provides a reduction of nitrogen oxides (NOx), as combustion takes place at temperatures far below those required for NOx formation [3]. Although Homogeneous Charge Compression Ignition (HCCI) and Premixed Charge Compression Ignition (PCCI) combustion are part of the Low-Temperature Combustion (LTC) strategy, their performance and flame stability remain limited. In contrast, Reactivity Controlled Compression Ignition (RCCI) strategy, which belongs to the LTC family, has garnered significant interest [4]. RCCI is a dual-fuel, partially premixed, combustion. This technic employs a low reactivity fuel, e.g. gasoline, methane, which is premixed with air prior being introduced into the combustion chamber. The mixture, air + low reactivity fuel, promotes homogeneity before the onset of ignition. Then, a small amount of high reactivity fuel, such as diesel, is injected during the compression stroke to ignite the mixture (Air + low reactivity fuel). This quantity is injected once or multiple times during the compression stroke. In this mode, the start of ignition delayed allowing for a better mixing.

Numerous studies have been conducted to meet the future requirements of clean and efficient combustion. Halis and Dogan. [5] analyzed the impact of intake air temperature in an RCCI engine fueled with iso-propanol and n-heptane. Their results concern the energy, exergy and sustainability analyses. A proportional correlation between intake air temperature and energy/exergy efficiency was identified. Nadimi et al. [6] studied, experimentally, dual fuel combustion using ammonia/diesel. Their work focused on combustion, emissions, and performances at different ammonia/diesel ratios. The results deliver 84.2% of input energy provided by ammonia. This percentage influences combustion duration and combustion phasing. The start of ignition is also retarded 8° compared to pure diesel case. Zhu et al. [7] applied an experimental and numerical studies of an RCCI Coal-to-liquid (CTL)/methanol combustion. The results were conducted under several loads. This study provided that the mixture methanol/CTL shortens the ignition duration for loads of 10%, 30% and 50%. Here, the reactivity gradient, inside the cylinder, increased from 28% to 451%

Published online: January 15 2025

proportionally to the engine load. Yousefi et al. [8] performed a numerical study regarding several premixed fuels (Methanol, natural gas and hydrogen) with diesel under several equivalence ratios (i.e., ϕ = 0.15, 0.2, 0.25, 0.3, and 0.35). For hydrogen/diesel, combustion experiences steeper pressure rises and the ignition timing advanced. For methane/diesel the location peak pressure retarded by 3.1 °CA. Methanol/diesel guaranteed an increase in the Indicated Mean Effective Pressure (IMEP) at equivalence ratio of ϕ= 0.35 compared to natural gas/diesel and hydrogen/diesel. Among these, the methanol/diesel combination provides the lowest combustion temperature, resulting in the lowest thermal NOx emissions. Nieman et al. [9] showed that using combinations of fuels ensures a large reactivity gradient, proportions between the high- and low-reactivity fuels. This combination, between dual fuels, controls combustion phasing and combustion duration. Domínguez et al. [10] experienced, experimentally, dual fuel combustion for two cases i.e; Diesel/Methanol and Diesel/Hydrogen. Their results carried out under low load and full load. The results proved hydrogen permits the substitution of 90% of diesel, although methanol failed to substitute diesel higher than 55 %.

Despite advancements, very scarce research adopted the impact of Natural gas/diesel equivalence ratio. The choice of natural gas and n-heptane mixture is due to the large reactivity gradient between them [9]. This reactivity makes it attractive for use in dual mode. Another driving force to accomplish Natural gas/diesel RCCI combustion is that methane's low reactivity allows for more mixing time before ignition.

This study adopts a range of equivalence ratio, ϕ = 0.3, 0.4, 0.5, 0.6, and 0.7. It is of importance to carry out an optimization of power and fuel consumption in an engine regime of 910 rpm. The high reactivity between the two fuels encourages coupling them. The low reactivity fuel (NG) serves at controlling the flame spread out of the high reactivity fuel (heptane). The results are carried out using ANSYS-forte. Forte allows combining chemical kinetics and computational fluid dynamics. The flow pattern is pursued using the Reynold Averaging Navier Stokes (RANS) approach. The RNG K-ε governs turbulence. The spray breakup is modeled using the hybrid Kelvin Helmholtz-Rayleigh Taylor. The simulations adopt the Eulerian-Lagrangian framework where gas is modeled as continuous media (Eulerian phase) and liquid spray is dispersed phase (Lagrangian). An in-depth focus is placed on combustion pattern, particularly, combustion phasing, ignition delay and ignition duration. These parameters reflect the evolution of combustion relative to Top Dead Center (TDC).

This paper consists of five sections. The section following the introduction highlights the modeling framework adopted. The employed configuration and boundary conditions are described in section 3. Section 4 is devoted to the results and discussions. Section 5 summarizes the main outcomes.

2. Computational Models

The SIMPLE solver is adopted as a solution algorithm where the governing equations are solved in sequence. With SIMPLE, known as segregated algorithm, the individual governing equations for the solution variables (e.g., u, v, w, p, T, etc) are solved one after another. Each governing equation, while being solved, is segregated from other equations. The numerical study steps are depicted in Fig. 1. It commences through drawing the computational geometry, then domain is discretized into multiple control volumes (mesh). To resolve the transport equations, boundary conditions and the main employed models are incorporated. The method is iterative, meaning the solution steps is iterated until a certain suitable convergence criterion is found. Post processing the results is afterwards addressed. The equations as well as source terms are deeply discussed starting subsection 2.1.

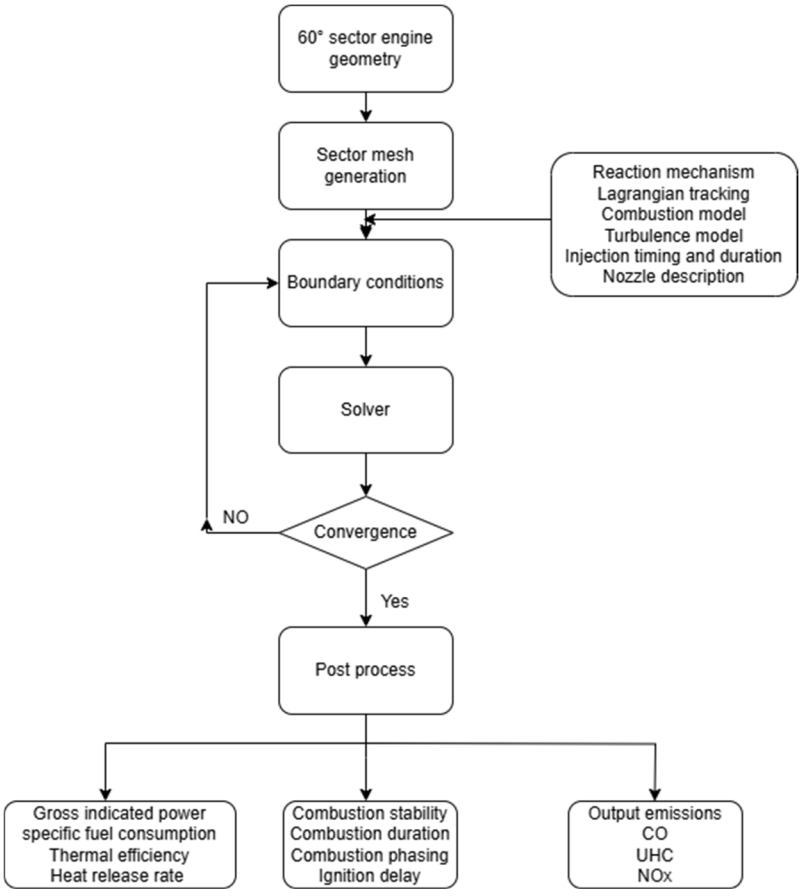

Fig. 1. Overview of the numerical scheme [11].

Table 1. Constants in the RNG $k-\varepsilon$ model [15].

	$C_{\varepsilon 1}$	C_s	$C_{\varepsilon 2}$	$C_{\varepsilon 3}$	$1/\mathrm{Pr}_k$	$1/\mathrm{Pr}_\varepsilon$
$k-\varepsilon$ RNG	1.42	1.5	1.68	–0.9 to 1.726	1.39	1.39

2.1. Gas-phase Eulerian equations

The governing equations for the mass, momentum and energy are calculated following the Eulerian framework. The continuity equation represents the rate of change in mass over time and space as follows [12, 13]:

$$\frac{\partial \bar{\rho}}{\partial t}+\nabla.(\bar{\rho}\tilde{u})=\dot{\bar{\rho}}^{s}, \tag{1}$$

the over bar $(\bar{})$ stands for the Reynolds, while tilde $(\tilde{})$ is for the Favre-averaging. The term $\dot{\bar{\rho}}^{s}$ represents the spray evaporation, $\tilde{u}$ is the Favre averaged velocity, while ρ denotes the density.

A turbulent flow of unit density, velocity $\tilde{u}$, pressure p, viscous shear stress tensor $\bar{\sigma}$, spray injection forces $\bar{F}^{s}$, gravitational force per unit volume ρg and the stress tensor that accounts for the effects of ensemble averaging Γ is assumed to be described as [12, 13]:

$$\frac{\partial \bar{\rho}\tilde{u}}{\partial t}+\nabla\cdot(\bar{\rho}\tilde{u}\tilde{u})=-\nabla\bar{p}+\nabla\bar{\sigma}-\nabla\cdot\Gamma+\bar{F}^{s}+\bar{\rho}\bar{g}, \tag{2}$$

To compute the impact of heat transfer, turbulent dissipation, turbulent transport, and chemical reactions, the internal energy transport equation read:

$$\frac{\partial \bar{\rho}\tilde{I}}{\partial t}+\nabla\cdot(\bar{\rho}\tilde{u}\tilde{I})=-\bar{p}\nabla\cdot\tilde{u}-\nabla\cdot\bar{J}-\nabla\cdot H+\bar{\rho}\tilde{\varepsilon}+\dot{\bar{Q}}^{C}+\dot{\bar{Q}}^{S} \tag{3}$$

here, I denotes the Internal energy, $\bar{p}$ represents the averaged pressure, J is derived from the total heat flux. The source terms $\dot{\bar{Q}}^{C}$ and $\dot{\bar{Q}}^{S}$ denote the production rate and the spray interaction, respectively. The quantity H is devoted for the effects of convection filtered term, while ε represents the dissipation rate.

The $(k-\varepsilon)$ RNG model is an updated turbulence model derived from the renormalization group theory. It enhances the standard $k-\varepsilon$ by incorporating additional terms in the dissipation rate (ε) equation to account for the effects of smaller-scale turbulence. The $k-\varepsilon$ RNG model serves as [14]:

$$\frac{\partial \bar{\rho}\tilde{k}}{\partial t}+\nabla\cdot(\bar{\rho}\tilde{u}\tilde{k})=-\frac{2}{3}\bar{\rho}\tilde{k}\nabla\cdot\tilde{u}+(\bar{\sigma}-\Gamma):\nabla\tilde{u}+\nabla\cdot\left[\frac{(\mu+\mu_T)}{\mathrm{Pr}_k}\nabla\tilde{k}\right]-\bar{\rho}\tilde{\varepsilon}+\dot{\bar{W}}^{S} \tag{4}$$

$$\frac{\partial \bar{\rho}\tilde{\varepsilon}}{\partial t}+\nabla\cdot(\bar{\rho}\tilde{u}\tilde{\varepsilon})=-(\frac{2}{3}c_{\varepsilon 1}-c_{\varepsilon 3})\bar{\rho}\tilde{\varepsilon}\nabla\cdot\tilde{u}+\nabla\cdot\left[\frac{\upsilon+\upsilon_T}{\mathrm{Pr}_\varepsilon}\nabla\tilde{\varepsilon}\right]+\frac{\tilde{\varepsilon}}{\tilde{k}}\left[c_{\varepsilon 1}(\sigma-\Gamma):\nabla\tilde{u}-c_{\varepsilon 2}\bar{\rho}\tilde{\varepsilon}+c_s\dot{\bar{W}}^{s}\right]-\bar{\rho}R \tag{5}$$

the model's coefficients Pr_k, Pr_ε, C_s, $C_{\varepsilon 1}$, $C_{\varepsilon 2}$ and $C_{\varepsilon 3}$ are highlighted in Table 1. The terms μ and μ_T represent the renormalized and the turbulence dynamic viscosity, respectively. The source term $\dot{\bar{W}}^{S}$ denotes the spray vaporization calculated by the Lagrange-formulation and Γ is the Reynolds stress tensor. Both υ and υ_T are the renormalized and the turbulent kinematic viscosity, respectively. R is related to the strain tensor.

2.2. Spray model

A solid-cone spray model, considering liquid breakup and subsequent drop atomization, is employed. The spray atomization follows the hybrid KH/RT model [16]. The spray disintegration occurs in three consecutive steps: 1) film formation at the nozzle exit, 2) sheet breakup, and 3) drop atomization. The liquid film is subject to aerodynamic instability that causes its breakup into liquid ligaments. The resulted drop are determined by drag, collision, turbulent dispersion, wall impingement, and secondary breakup [17].

2.3. Injection timing and duration

To control the fuel reactivity and combustion phasing, RCCI approach aims at blending two fuels. The fuels, natural gas/heptane, differences are volatility, influencing mixing, and reactivity, which effect the ignition delay [26]. Once the mixture, air/natural gas, is introduced into the combustion chamber, diesel injection is afterwards established. Here, its timing and duration are 22° BTDC and 6.11°, respectively.

2.4. Chemistry model

A N-heptane reaction mechanism, consisting of 425 total species and 3128 reactions, is employed to model the diesel-methane chemistry. The mechanism was validated by simulating the ignition delay of N-heptane under constant volume at various initial conditions [18]. Numerical simulations are conducted by using the software ANSYS-Forte. Forte enables the simulation of combustion processes by incorporating a n-heptane reaction mechanism. In engine combustion, it is known that the fuel and the oxidizer do not have enough time to mix down into molecular level [17]. This leads to inevitable inhomogeneities. This inhomogeneities is caused by a partial mixing of combustion radicals and products during the combustion. Therefore, the reactions might be partly controlled by the breakup of turbulent eddies. The employed model incorporates the turbulent mixing in conjunction with the reaction rate of each species [19]. This model is deduced as:

$$\dot{\bar{\omega}}_{k,eff}=\frac{Y_{k,EQ}-Y_k}{\tau_{eff}} \tag{6}$$

where $\dot{\bar{\omega}}_{k,eff}$ is the production rate of k^{th} species. The quantity Y_k represents the instantaneous concentration of the k species and $Y_{k,EQ}$ denotes the equilibrium concentration.

The effective time scale, τ_{eff}, is related to the chemical time scale τ_{chem} and the diffusive turbulent mixing time scale τ_{mix} as:

$$\tau_{eff} = \tau_{chem} + \tau_{mix} \tag{7}$$

the turbulent timescale τ_{mix} is the eddy turnover time. It is proportional to k / ε.

The summation of $\dot{\omega}_{k,eff}$ is incorporated in the species conservation equation. To omit the mol unit, this quantity is multiplied to the molecular weight W_k of k species and written as:

$$\dot{\rho}_k^c = W_k \sum_{i=1}^{I} \dot{\omega}_{ki} \tag{8}$$

The species conservation equation is then found as [13]:

$$\frac{\partial \overline{\rho}_k}{\partial t} + \nabla.(\overline{\rho}_k \overline{u}) = \nabla.[\overline{\rho} D \nabla y_k] + \nabla.\Phi + \dot{\rho}_k^c + \dot{\rho}_k^s \tag{9}$$

here, ρ and its subscript k are the density and species index, respectively. $\overline{u}$ is the flow mean velocity and $y_k = \rho_k / \rho$ is the mass fraction of species. D is the molecular diffusion coefficient. The term Φ accounts for the impact of the ensemble-averaging of the convection term. Both $\dot{\overline{\rho}}_k^c$ and $\dot{\overline{\rho}}_k^s$ denote the source term due chemical reactions and spray evaporation, respectively.

3. Computational Domain and Boundary Conditions

RCCI mode is adopted as a Low Temperature Combustion (LTC) mode. It provides combustion in regions away from high-temperature zones where NOx formed. RCCI typically employs two fuels, as highlighted in Fig. 2. The first fuel, low reactive, is introduced inside the combustion chamber premixed with air. It retards the start of ignition encouraging better mixing. A little second high reactive fuel quantity, e.g. diesel, is injected during the compression stroke, when piston reach near the Top Dead Center (TDC), to ignite the mixture.

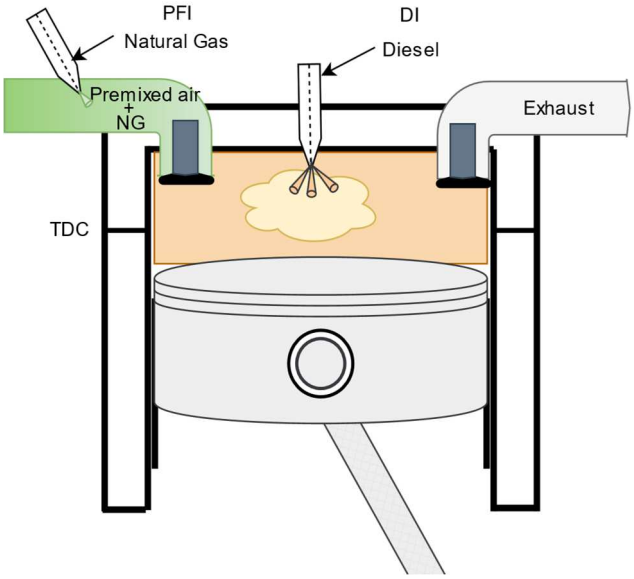

Fig. 2. Schematic illustration of RCCI working principle.

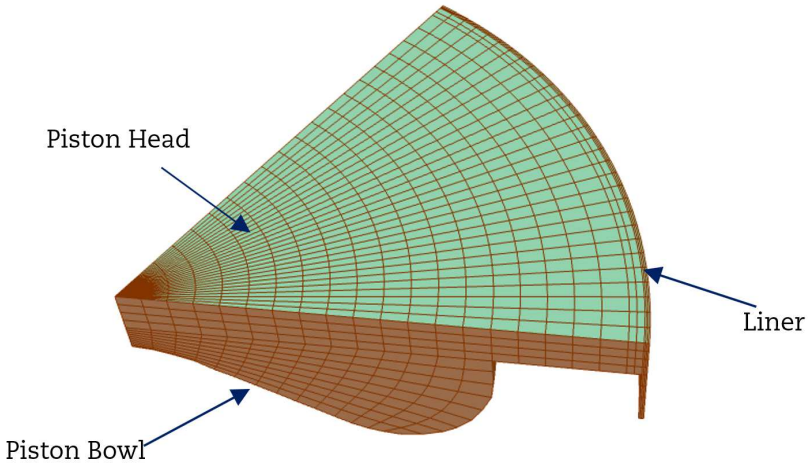

Fig. 3. Computational grid.

Table 2. Numerical models.

Physical process	Model
Turbulence model	RNG k-ε
Spray breakup model	KH-RT
Laminar flame speed	Power Law
Turbulent flame speed	Peters model
NOx model	Zeldovich

Table 3. Engine specification.

Operating Condition	Value
Bore × stroke [mm × mm]	137.16 × 165.1
Engine speed [rpm]	910
IVC [°CA]	190
EVO [°CA]	505
Hole diameter [mm]	0.23
SOI [°CA BTDC]	23
Compression ratio [-]	16.25
Spray cone angle [°]	10

Table 4. Initial and boundary conditions.

Boundary conditions	Boundary type/ specific condition
Cylinder head temperature [K]	400
Piston temperature [K]	400
Liner temperature [K]	400
Initial conditions	
Pressure at IVC [bar]	1.02
Temperature at IVC [K]	360
Turb. Kin. Energy [m^2/s^2]	10
Turb. Length scale [m]	0.003

The model utilized in simulating the five cases is exhibited in Fig. 3. The computational model consists of 60° periodic sector mesh, corresponding to a single hole of the six-holes injector. This approach is based on a hypothesis of a periodic phenomenon in each 60° (each hole fuels 60° sector). It is cost-effective, resulting to a decrease in computational time. The computational domain, with periodic boundaries, is discretized using the quadratic elements. This regular mesh permits data management easy during computation, where data smoothly transferred through cells. Here, the mesh is dynamic following a layering technique. For the spray atomization, the grid-independent spray breakup model of Abani et al. [20], called the gas-jet model, was employed. The employed models are listed in Table 2.

The engine specifications are taken from experiments of Yousefi et al. [21]. Table 3 provides the main specifications needed for simulations. The boundary and initial conditions, in Table 4, are adopted in resolving the transport equations. The same conditions were utilized by Hamdi at al. [12]. Their results were in better agreement with the experiment.

4. Results and Discussions

4.1. Validation

This study is validated against experimental work of Yousefi et al. [21]. Validation, in Fig. 4, regards the pressure and heat release rate. The simulations are found to be able in capturing the combustion characteristics well. The start of ignition as well as ignition duration of HRR corresponds to the same crank angle positions of the HRR. The discrepancy related to pressure is a little bit over predicted. The discrepancy, at 357° BTDC, associated with HRR can be attributed to the quality of air/fuel mixing in molecular level.

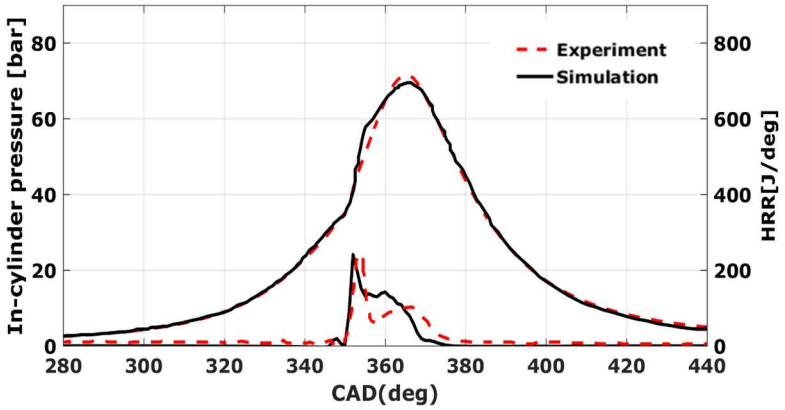

Fig. 4. Comparison of measured and predicted pressure and heat release rate.

Table 5. Parametric study.

	$\dot{m}_{air}$	$\dot{m}_{diesel}$	$\dot{m}_{Natural\ gas}$	Equivalence ratio ϕ
1			0.76 kg/h	ϕ = 0.3
2			1.306 kg/h	ϕ = 0.4 (Validated against experiment [21])
3	67.57 kg/h	0.471 kg/h	1.55 kg/h	ϕ = 0.5
4			1.88 kg/h	ϕ = 0.6
5			2.34 kg/h	ϕ = 0.7

4.2. Baseline cases

Equivalence ratio serves as the mass ratio of the theoretical air required for completely combustion (Stoichiometric) of the fuel injected into the cylinder. The present work performs five different equivalence ratios i.e. ϕ = 0.3, 0.4, 0.5, 0.6 and 0.7. Here, combustion is conducted under lean condition following eq.10. The calculation is based upon previous study conducted by Zheng et al. [22] and Daneh-Dezfuli et al. [23]. A ϕ = 0.4 is validated against experiment [21]. This calculation conserves the quantity of liquid diesel. The amount of natural gas is adjusted for each equivalence ratio. The mass flow rate of both fuels and air are illustrated in Table 5.

$$\Phi = \frac{\dot{m}_{gas} \times AFR_{gas} + \dot{m}_{diesel} \times AFR_{diesel}}{\dot{m}_{air}} \tag{10}$$

AFR represents the air fuel ratio. The quantity $\dot{m}$ is the mass flow rate. In RCCI, combustion is partially premixed. Using a lean equivalence ratio ensures a greater amount of oxidizer relative to the fuel, resulting to better interaction between them.

The quantity ϕ is incorporated in the natural gas species transport equation. The rate of change of natural gas mass fraction, y_{NG}, with respect to cell volume serves, in Eq. (11), as follow [24]:

$$\frac{dy_{NG}}{dt} = \upsilon \dot{\omega}_{NG} \cdot W_{NG} \tag{11}$$

where υ denotes the cell volume, $\dot{\omega}_{NG}$ represents the production rate of natural gas, and W_{NG} is the molecular weight.

4.3. Engine performances over a range of equivalence ratio

Figure 5 displays the temperature contours for various equivalence ratios. Worth to note that the temperature is recorded on a cut plane coincident with the spray jet axis. It is registered that the flame starts on/near the piston bowl. It is caused by the mixed convection/conduction heat transfer mode. The high-temperature in near bowl increases piston bowl heat transfer and therefore, reduced the thermal efficiency [18]. For $0.4 \leq \phi \leq 0.6$, the ignition area is roughly similar. For ϕ = 0.7, it is inferred the start of ignition delays to 10° ATDC. This is explained by the fact of the excess of low reactivity fuel, natural gas ratio, that extends the ignition timing.

Turbulent kinetic energy is a quantitative measure of turbulence intensity for a given flow. Outlining TKE is insightful since this latter affords the diffusive mixing. It is also relevant in characterizing the in-cylinder location where turbulence being created. Here, the TKE is generated during combustion stroke at TDC, 5° ATDC and 10° ATDC, and reported in Fig. 6. It is observed that TKE decreases as the piston moves down to the bottom dead center. For $0.3 \leq \phi \leq 0.5$, the same area is roughly covered. The TKE starts on/near piston bowl then it flows out through the whole volume. This quantity penetrates the squish region and the near cylinder liner. For ϕ = 0.7 at 10° ATDC, the TKE remains extensive. It is related to the retarded start of ignition.

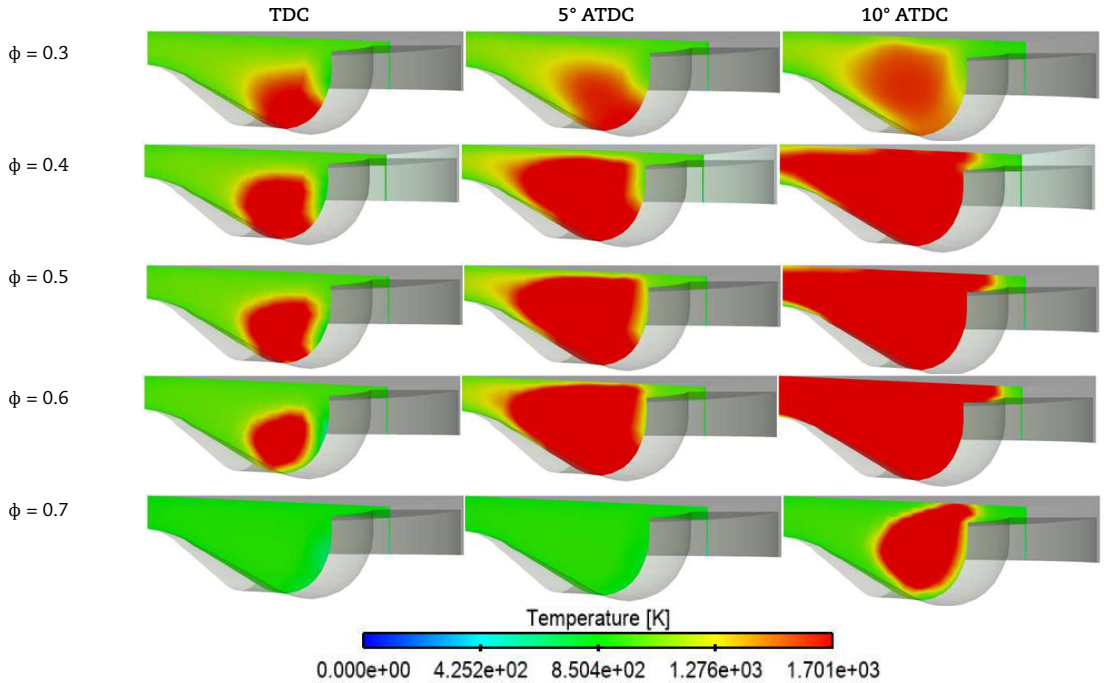

Fig. 5. In-cylinder temperature contours, coincident with the spray axis.

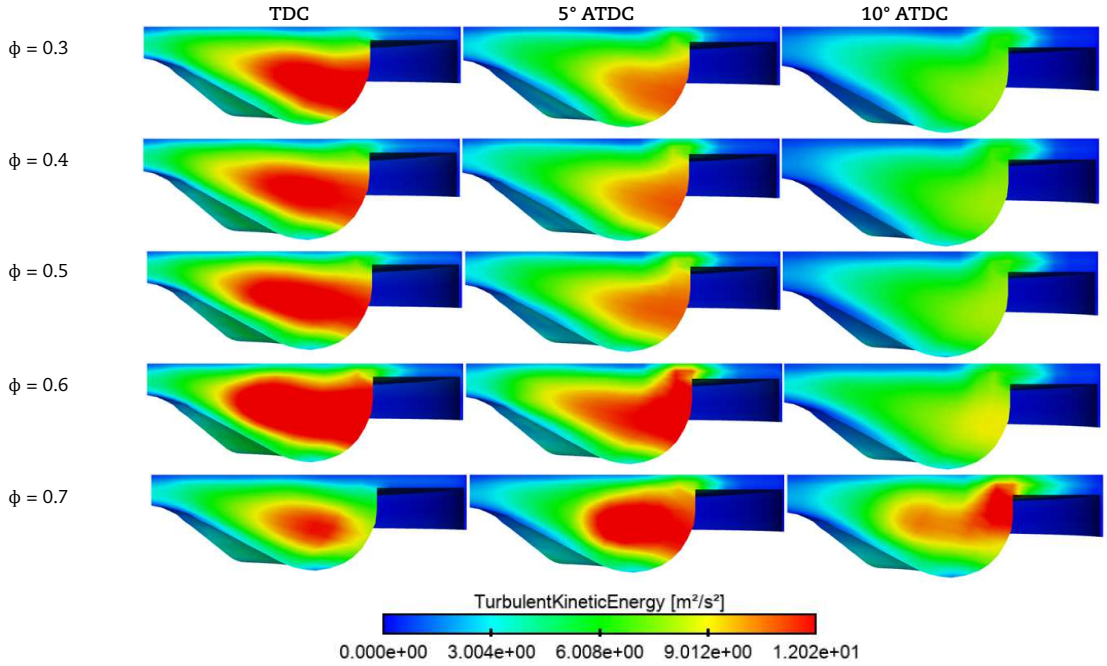

Fig. 6. Turbulent kinetic energy contours at 0°, 5° and 10° ATDC.

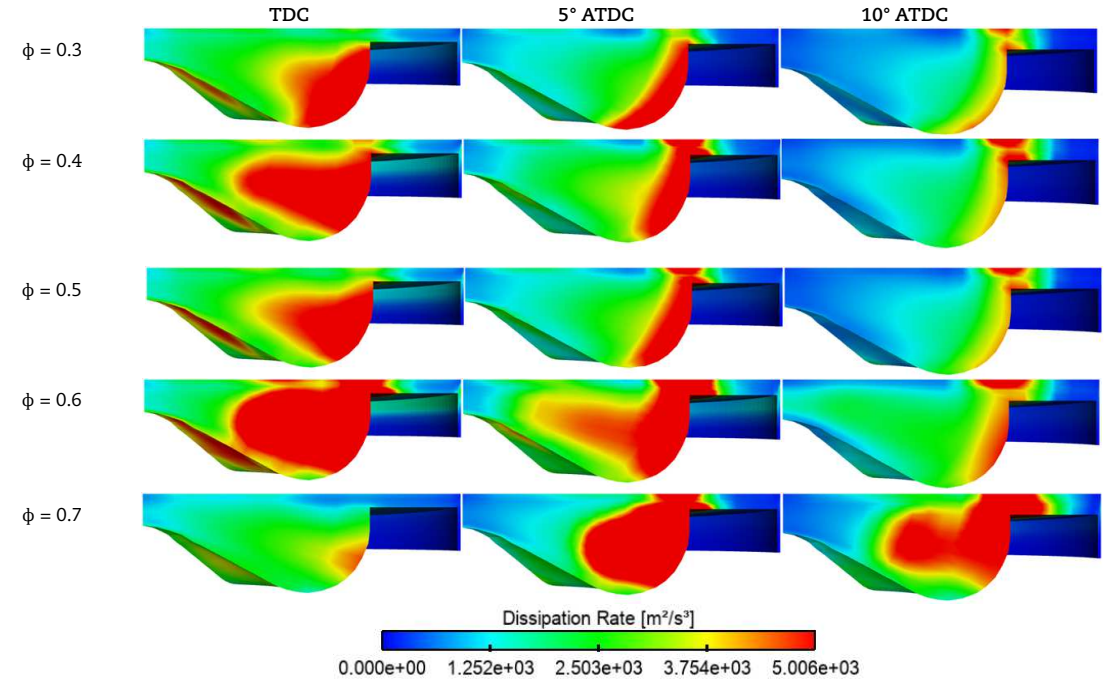

Fig. 7. Dissipation rate of the turbulent kinetic energy contours at 0°, 5° and 10° ATDC.

The dissipation rate is a key parameter to quantify the level of turbulence, and therefore the resulted mixing [25]. The dissipation rate of the turbulent kinetic energy elucidates how fast the turbulent eddies entirely dissipate within the volume. It is related to turbulent eddies length scale. Worth noting, the larger the eddy, the higher the TKE. In Fig. 7, for $0.3 \leq \phi \leq 0.5$, the amount of energy starts dissipated at TDC. The gradient of the turbulent kinetic energy has rapidly vanished near the piston bowl, squish and cylinder head.

Pressure evolution versus crank angle is displayed in Fig. 8. For $0.3 \leq \phi \leq 0.6$, the pressure is proportionally correlated with equivalence ratio. It increases as the equivalence ratio rises. For $\phi = 0.7$, the pressure is remarkably decreased though, the combustion duration is increased. The maximum pressure is found at 372°. The peak value, for $\phi = 0.7$, is retarded 6° compared to $\phi = 0.4$, 0.5, and 0.6. At this level, for $\phi = 0.7$, natural gas negatively impacts the pressure, leading to a downward trend. Similar drop has been found by Zheng et al. [22].

Figure 9 shows that for $\phi = 0.3$, the combustion is advanced and starts at 348°. It is due to the high heptane reactivity, which is the dominant quantity. For $0.4 \leq \phi \leq 0.5$, the ignition occurs twice, where the second peak is controlled by diffusion rather than kinetic [26]. It means the flame propagation is not limited to the ignition chemistry, although the turbulence diffusive term. The highest peak displayed at $\phi = 0.6$, is related to the optimal reactivity between heptane and natural gas under this load. Increasing the natural gas ratio postpones the start of ignition. This is particularly evident for $\phi = 0.7$, indicating that natural gas, a low-reactivity fuel, governs the combustion process [22]. Low cetane number could be a major factor in retarding the onset of ignition [27].

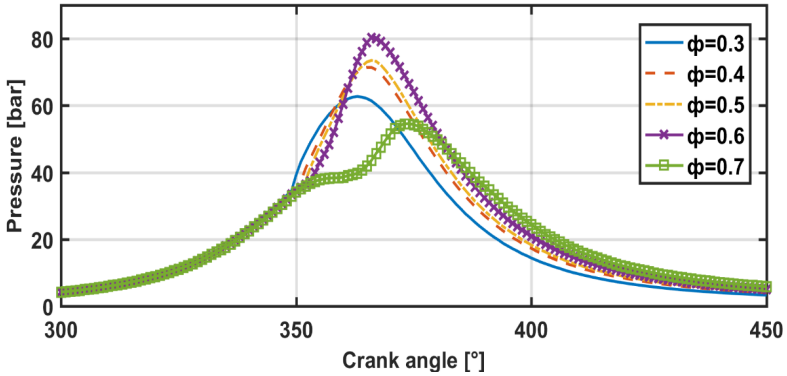

Fig. 8. In-cylinder pressure of natural gas/diesel dual-fuel strategy at various equivalence ratios.

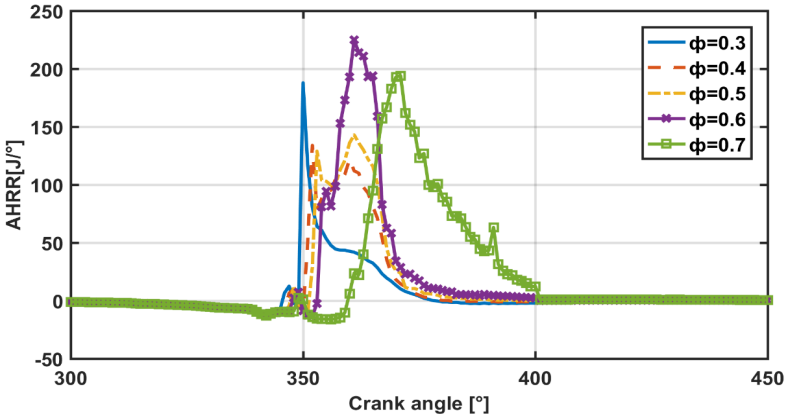

Fig. 9. Apparent heat release rate.

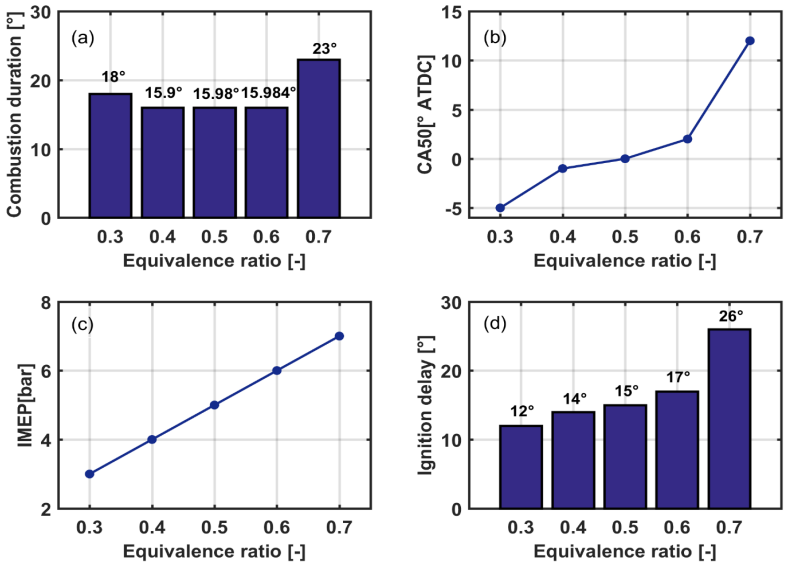

Fig. 10. Combustion pattern in term of (a) Combustion duration; (b) Combustion phasing (CA50); (c) Indicated Mean Effective Pressure (IMEP); and (d) Ignition delay.

The bar chart, Fig. 10(a), highlights the combustion duration as function of crank angle for the various equivalence ratio. The combustion duration is recorded by integrating the total heat released from CA10% to CA90%. For $0.4 \leq \phi \leq 0.6$, the duration is approximately equal regardless the combustion process pattern. For $\phi = 0.7$, the combustion yields a prolonged duration. It is explained by the fact of the high natural gas ratio. Noting that large reactivity gradient aids also in extending the combustion duration. Figure 10(b) displays for each equivalence ratio the standard deviation of CA50(°ATDC), representing the crank angle at which 50% of total heat released. It is employed as an indicator of the combustion phasing. It is observed varying the equivalence ratio impacts CA50. For the studied range, $0.3 \leq \phi \leq 0.6$, an increased change in combustion phasing (CA50) is noticed. For $\phi = 0.7$, the delay in location of CA50, by 12°ATDC, is correlated to the fact of the low reactivity between the premixed (Natural gas-air) and the injected fuel [28]. In Fig. 10(c), the Indicated Mean Effective Pressure (IMEP), reflects the several engine load. It is the integral of the pressure-volume evolution divided by the volume of the cylinder. Here, the output IMEP is linearly increased with equivalence ratios increasing. For $\phi = 0.6$ (6 bar IMEP), the CA50 coincides with 2°, though experiment CA50 ranges between 4 and 6° [2]. This low reactivity delays the start of ignition, as shown in Fig. 10(d).

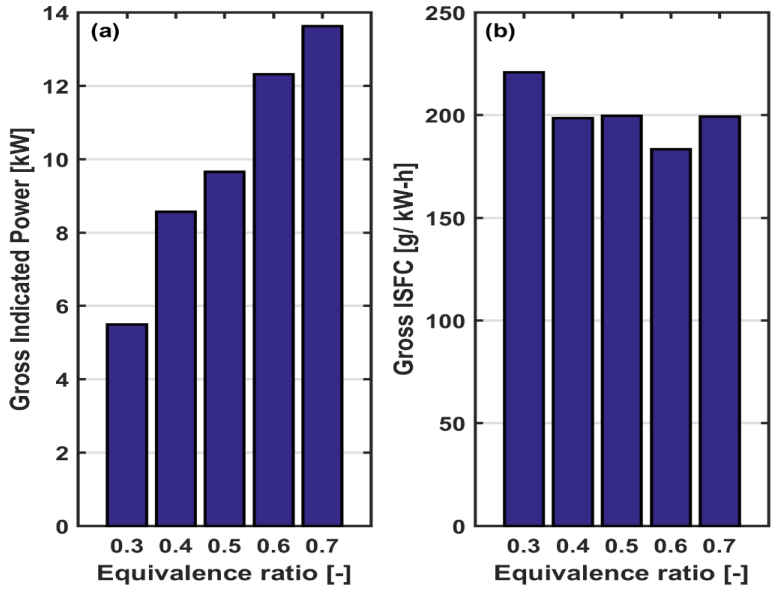

Fig. 11. Engine performances: (a) Gross Indicated Power; (b) Specific fuel consumption.

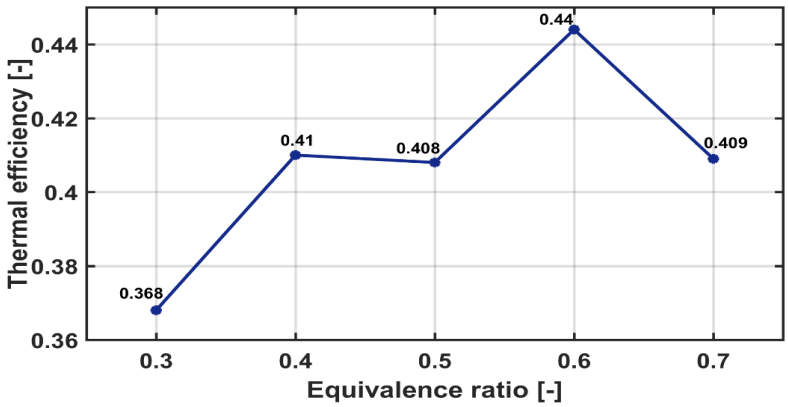

Fig. 12. Effect of equivalence ratio in engine thermal efficiency.

In Fig. 11, both the gross indicated power and Indicated Specific Fuel Consumption (ISFC) are reported. The gross indicated power is proportionally correlated to the equivalence ratio. This is because a high equivalence ratio yields a greater quantity of energy. The lower fuel consumption found to lies at $\phi = 0.6$. For $\phi \geq 0.7$, the specific fuel consumption increases. This is most likely due to the insufficient mixing of the oxidizer throughout the entire cylinder. The best operating condition at 910 rpm, achieving the lowest fuel consumption, is $\phi = 0.6$.

The engine efficiency is calculated following Eq. (12) as given by Kokjohn et al. [18]. Here, thermal efficiency varies for various NG energy, as registered in Fig. 12. Efficiency is found maximum at $\phi = 0.6$, leading to an increase of 7% compared to experiment ($\phi = 0.4$). For $\phi = 0.7$, a downward trend is found, which is very likely due to the postponed start of ignition in conjunction with the wide ignition duration (Figs. 11(a) and (b)). The flammability limit is expected to affect the thermal efficiency when the equivalence ratio (ϕ) is 0.3. A previous studies of Liang and Law. [29] and Bertolino et al. [30], studied diesel and heptane detailed chemistry (representing diesel), prove that temperature reach its minimum at $\phi = 0.3$:

$$\eta_{th} = \frac{W}{m_{fuel} \times LHV_{fuel} \times \eta_{comb}} \tag{12}$$

where W represent the indicated work. The quantities m_{fuel} and LHV_{fuel} are the mass of the fuel and the averaged lower heating value, respectively. The averaged LHV is assumed 44 MJ/kg and η_{comb} serves combustion efficiency.

4.4. Output emissions

Unburned hydrocarbons at exhaust valve opening, are recorded in ppm unit. Hydrocarbons accounts all species that have nonzero atoms of both H and C. Unburned hydrocarbon is calculated as:

$$UHC[ppm] = 10^6 \times \sum_{\text{Species Containing C,H Elements Only}} nc_i x_i \tag{13}$$

where nc_i denotes the number of carbon atoms per molecule and x_i represents the mole fraction of species i.

Combustion with $\phi = 0.6$, outlined in Fig. 13, produces the lowest UHC quantity. The highest UHC is denoted at $\phi = 0.4$. The primary cause of high levels of unburned hydrocarbons (UHC) is argued to low combustion temperature. This is, particularly, found when liquid fuel entering crevice regions and the cylinder liner [18]. This phenomenon is detected in the temperature contour shown in Fig. 5.

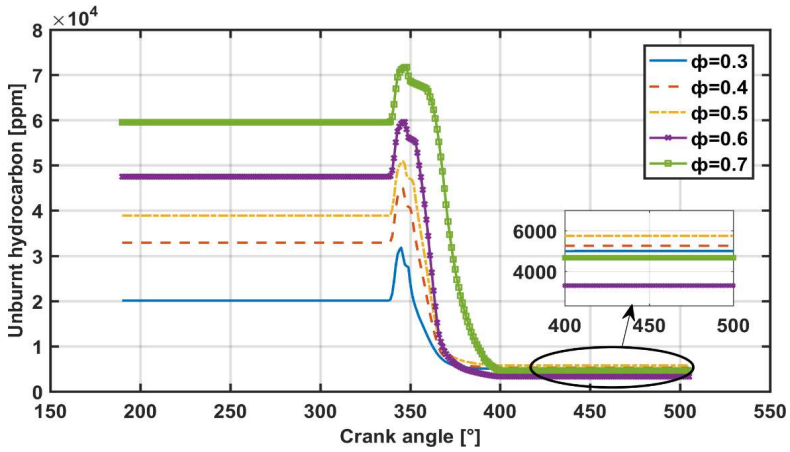

Fig. 13. Unburned hydrocarbon.

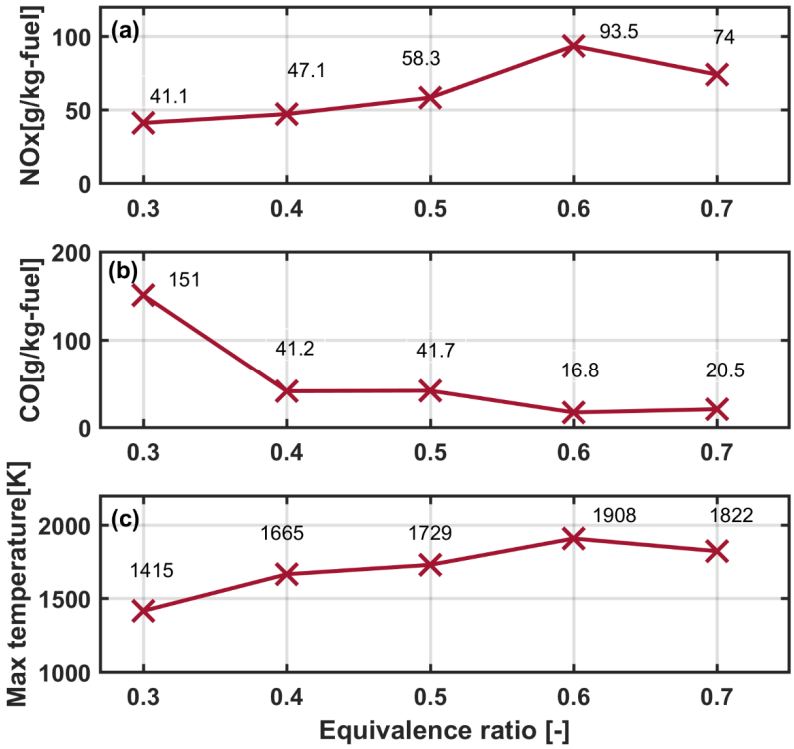

Fig. 14. Evolution of (a) NOx at EVO; (b) CO_2 at EVO; (c) In-cylinder maximum temperature.

Since the consequent emissions are highly related to the encountered temperature, CO, and NOx are highlighted in conjunction with in-cylinder maximum temperature as shown in Fig. 14. For $0.3 \leq \phi \leq 0.6$, the trend of NOx emissions continues to rise, reaching up to 93.5 g/kg-fuel. This increase corresponds with the maximum temperature, indicating the NOx produced are primarily thermal. NOx emissions decrease with leanest mixture, $\phi = 0.3$, due to the low associated combustion temperature [31]. Carbon monoxide (CO) is mainly generated when the gas temperature is not sufficiently high for CO to oxidize. This quantity of CO is immense for $\phi = 0.3$. It is roughly nine times higher compared to $\phi = 0.6$ (Lowest CO). For $\phi = 0.3$, combustion reach the lean flammability limit of Natural gas/diesel.

5. Conclusion

The effect of a wide range of lean equivalence ratio, varying from $0.3 \leq \phi \leq 0.7$, on the combustion performances and emissions was studied. The choice of lean mixture was to control the flame temperature that inhibits thermal NOx formation. The objective of this work is to reduce NOx, UHC and CO emissions, while improving/keeping the gross indicated power. This work followed the Eulerian-Lagrangian framework. The main concluding remarks are listed below.

- For $0.3 \leq \phi \leq 0.6$, the lower equivalence ratio corresponds to the higher concentration of unburned hydrocarbons. This is attributed to the fact that a lower equivalence ratio approaches the flammability limit of Heptane/Natural Gas. Flammability limit results in incomplete combustion and a greater presence of unburned hydrocarbons.
- Gross Indicated power increases proportional with the equivalence ratio while the gross ISFC is shown to remain minimum at $\phi = 0.6$. It reduces 8% relative to $\phi = 0.4$ (validates experiment). This latter, gross ISFC, ensures the optimum combustion under the engine regime of 910 rpm.
- The ignition delay increases proportionally with the equivalence ratio. This, in turn, delays the CA50 (the crank angle at which 50% of the fuel has burned). The high auto-ignition temperature of natural gas is a major factor impacts this delay. A

longer combustion delay leads to a build-up the fuel and air mixture. It results in an unstable flame once ignition starts.

- Natural gas substitution retards the start of combustion at a given mass level. It is denoted at $0.6 \leq \phi \leq 0.7$. The CA50 (combustion phasing) is found to lie at 12° ATDC for $\phi = 0.7$, caused by the low reactivity of natural gas.
- For the range $0.3 \leq \phi \leq 0.6$, increasing the equivalence ratio augments maximum temperature. The maximum temperature, in turn, results in an increase in NOx, revealing the primary quantity of NOx is thermal.
- The impact of natural gas substitution on CO emissions varies along with the equivalence ratio. For $\phi = 0.3$, CO emissions are elevated. Maximum temperature is low, indicating an incomplete combustion. Increasing natural gas mass fraction decreases CO species roughly 9 times. The lowest emission is observed at $\phi = 0.6$.
- For $\phi = 0.6$, an increase of 15% in temperature compared to experimental work ($\phi = 0.4$). This change in temperature is followed by a decrease in CO by 6%.
- For $\phi = 0.3$, the UHC is determined to diminish 27% compared to experiment. It depends on the impact of flammability limit of very lean mixture.

Author Contributions

The authors have confirmed their contributions to this study as follows: F. Hamdi was responsible for formal analysis and drafting the original manuscript; H. Wassim contributed to formal analysis and editing the original draft; and M. Chrigui oversaw conceptualization and supervision. The manuscript was written through the contribution of all authors. All authors discussed the results, reviewed, and approved the final version of the manuscript.

Acknowledgments

Not applicable.

Conflict of Interest

The authors declared no potential conflicts of interest concerning the research, authorship, and publication of this article.

Funding

Not applicable.

Data Availability Statements

Not applicable.

Nomenclature

AHRR	Apparent Heat Release Rate	IVC	Intake Valve Closing
ATDC	After Top Dead Center	KH-RT	Kelvin Helmholtz-Rayleigh Taylor
BTDC	Before Top Dead Center	LHV	Lower Heating Value
CA	Crank Angle	LNT	Lean NO_x Trap
CA50	Combustion phasing	LTC	Low Temperature Combustion
CFD	Computational Fluid Dynamics	NG	Natural Gas
CI	Compression Ignition	NO_x	Nitrogen Oxide
CO	Carbon monoxide	PCCI	Premixed Charge Compression Ignition
CO_2	Carbon dioxide	RANS	Reynolds Averaging Navier Stokes
DOI	Duration Of Injection	RM	Reaction Mechanism
DPF	Diesel Particulate Filter	RNG	Re-Normalization Group
EVO	Exhaust Valve Opening	RCCI	Reactivity Controlled Compression Ignition
HCCI	Homogeneous Charge Compression Ignition	SCR	Selective Catalytic Reduction
ICE	Internal Combustion Engine	SOI	Start Of Injection
IMEP	Indicated Mean Effective Pressure	TDC	Top Dead Center
ISFC	Indicated Specific Fuel Consumption	UBHC	Unburned Hydrocarbon

References

[1] Hamdi, F., Nouri, H., Labiadh, Z., Agrebi, S., Chrigui, M., Sadiki, A., Experimental study for selective reduction of NOx from diesel engine exhaust gases at low temperature using activated carbon, *Water, Air, & Soil Pollution*, 233, 2022, 327.
[2] Reitz, R.D., Duraisamy, G., Review of high efficiency and clean reactivity controlled compression ignition (RCCI) combustion in internal combustion engines, *Progress in Energy and Combustion Science*, 46, 2015, 12–71.
[3] Turns, S.R., *An introduction to combustion: concepts and application*, 2nd edition, 1999.
[4] Kokjohn, S.L., Hanson, R.M., Splitter, D.A., Reitz, R.D., Experiments and modeling of dual-fuel HCCI and PCCI combustion using in-cylinder fuel blending, *SAE International Journal of Engines*, 2, 2010, 24–39.
[5] Halis, S., Dogan, B., Effects of intake air temperature on energy, exergy and sustainability analyses in an RCCI engine fueled with iso-propanol and n-heptane, *Energy*, 284, 2023, 129050.
[6] Nadimi, E., Przybyła, G., Lewandowski, M.T., Adamczyk, W., Effects of ammonia on combustion, emissions, and performance of the ammonia/diesel dual-fuel compression ignition engine, *Journal of the Energy Institute*, 107, 2023, 101158.
[7] Zhu, J., Wang, Z., Li, R., Liu, S., Li, M., Experimental and simulation study of methanol/coal-to-liquid (CTL) reactivity and combustion characteristics of diesel engines in RCCI mode, *Fuel*, 357, 2024, 129799.
[8] Yousefi, A., Birouk, M., Lawler, B., Gharehghani, A., Performance and emissions of a dual-fuel pilot diesel ignition engine operating on various premixed fuels, *Energy Conversion and Management*, 106, 2015, 322–336.

[9] Nieman, D.E., Dempsey, A.B., Reitz, R.D., Heavy-duty RCCI operation using natural gas and diesel, *SAE International Journal of Engines*, 5, 2012, 270–285.
[10] Domínguez, V.M., Hernández, J.J., Ramos, Á., Reyes, M., Rodriguez-Fernandez, J., Hydrogen or hydrogen-derived methanol for dual-fuel compression-ignition combustion: An engine perspective, *Fuel*, 333, 2023, 126301.
[11] Bayramoglu, K., Yılmaz, S., Emission and performance estimation in hydrogen injection strategies on diesel engines, *International Journal of Hydrogen Energy*, 46, 2021, 29732–29744.
[12] Hamdi, F., *et al.*, Impact of spray cone angle on the performances of methane/diesel RCCI engine combustion under low load operating conditions, *Entropy*, 24, 2022, 650.
[13] Mondo, K., Agrebi, S., Hamdi, F., Lakhal, F., Sadiki, A., Chrigui, M., Impact of multi-component surrogates on the performances, pollutants, and exergy of IC engines, *Entropy*, 24, 2022, 671.
[14] Han, Z., Reitz, R.D., Turbulence modeling of internal combustion engines using RNG k-ε models, *Combustion Science and Technology*, 106, 1995, 267–295.
[15] Yakhot, V., Orszag, S.A., Renormalization group analysis of turbulence. I. Basic theory, *Journal of Scientific Computing*, 1, 1986, 3–51.
[16] Beale, J., Reitz, R., Modeling spray atomization with the KH-RT hybrid model, *Atomization and Sprays*, 9, 1999, 623–650.
[17] Kong, S.C., Reitz, R.D., Application of detailed chemistry and CFD for predicting direct injection HCCI engine combustion and emissions, *Proceedings of the Combustion Institute*, 29, 2002, 663–669.
[18] Kokjohn, S.L., Hanson, R.M., Splitter, D.A., Reitz, R.D., Fuel reactivity controlled compression ignition (RCCI): A pathway to controlled high-efficiency clean combustion, *International Journal of Engine Research*, 12, 2011, 209–226.
[19] Kong, S.C., Reitz, R.D., Use of detailed chemical kinetics to study HCCI engine combustion with consideration of turbulent mixing effects, *Journal of Engineering for Gas Turbines and Power*, 124, 2002, 702–707.
[20] Abani, N., et al., An improved spray model for reducing numerical parameter dependencies in diesel engine CFD simulations, *SAE Technical Paper*, 2008-01-0970, 2008.
[21] Yousefi, A., Birouk, M., Guo, H., An experimental and numerical study of the effect of diesel injection timing on natural gas/diesel dual-fuel combustion at low load, *Fuel*, 203, 2017, 642–657.
[22] Zheng, J., Wang, J., Zhao, Z., Wang, D., Huang, Z., Effect of equivalence ratio on combustion and emissions of a dual-fuel engine, *Applied Thermal Engineering*, 146, 2019, 738-751.
[23] Daneh-Dezfuli, A., Khamisi, S., Bahrainian, S.S., Numerical analysis of preheating furnace performance in Razi Petrochemical's ammonia processing unit considering the effects of hydraulic and geometric variables, *Journal of Applied and Computational Mechanics*, 2024, doi: 10.22055/jacm.2024.46917.4624.
[24] Kokjohn, S.L., *Reactivity controlled compression ignition (RCCI) combustion*, University of Wisconsin–Madison, USA, 2012.
[25] Wang, G., *et al.*, Estimation of the dissipation rate of turbulent kinetic energy: A review, *Chemical Engineering Science*, 229, 2021, 116133.
[26] Wissink, M., Reitz, R., Exploring the role of reactivity gradients in direct dual fuel stratification, *SAE International Journal of Engines*, 9, 2016, 1036–1048.
[27] Shahsavan, M., Morovatiyan, M., Mack, J.H., A computational investigation of non-premixed combustion of natural gas injected into a mixture of argon and oxygen, *ASME International Combustion Engine Division Fall Technical Conference (ICEF)*, 2018, doi: 10.1115/ICEF2018-9618.
[28] Dempsey, A.B., Walker, N.R., Gingrich, E., Reitz, R.D., Comparison of low-temperature combustion strategies for advanced compression ignition engines with a focus on controllability, *Combustion Science and Technology*, 186, 2014, 210–241.
[29] Liang, W., Law, C.K., Extended flammability limits of n-heptane/air mixtures with cool flames, *Combustion and Flame*, 185, 2017, 75–81.
[30] Bertolino, A., Stagni, A., Cuoci, A., Faravelli, T., Parente, A., Frassoldati, A., Prediction of flammable range for pure fuels and mixtures using detailed kinetics, *Combustion and Flame*, 207, 2019, 120–133.
[31] Kuppa, K., Nguyen, H.D., Goldmann, A., Korb, B., Wachtmeister, G., Dinkelacker, F., Numerical modeling of unburned hydrocarbon emissions in gas engines with varied fuels, *Fuel*, 254, 2019, 115532.

ORCID iD

Fathi Hamdi https://orcid.org/0000-0003-1404-1973
Wassim Harizi https://orcid.org/0009-0008-9880-4213
Mouldi Chrigui https://orcid.org/0000-0002-2775-6436

How to cite this article: Hamdi F., Harizi W., Chrigui M. RANS Study on the Impact of Equivalence Ratio on Natural Gas/Diesel-Fueled Combustion in RCCI Engine, *J. Appl. Comput. Mech.*, 11(4), 2025, 1075-1086.
https://doi.org/10.22055/jacm.2025.47683.4763